Molecular Mobility and Nucleocytoplasmic Flux in Hepatoma Cells

Iphigenie Lang, Manfred Scholz, and Reiner Peters

Max-Planck-Institut für Biophysik, 6000 Frankfurt 70, Federal Republic of Germany

Abstract. Fluorescence microphotolysis (photobleaching) was used to measure, in single polyethylene glycol–induced polykaryons of hepatoma tissue culture cells, nucleocytoplasmic flux and intracellular mobility for a series of dextrans ranging in molecular mass from 3 to 150 kD and for bovine serum albumin.

For the dextrans, the cytoplasmic and the nucleoplasmic translational diffusion coefficients amounted to ~9 and ~15%, respectively, of the value in dilute buffer. The diffusion coefficients depended inversely on molecular radius, suggesting that diffusion was dominated by viscosity effects. By application of the Stokes-Einstein equation, cytoplasmic and nucleoplasmic viscosities were derived to be 6.6 and 8.1 cP, respectively, at 23°C. Between 10 and 37°C nucleoplasmic diffusion coefficients increased by ~45–85%, whereas cytoplasmic diffusion coefficients were virtually independent of temperature. In contrast to that of the dextrans, diffusion of bovine serum albumin was more restricted. In the cytoplasm the diffusion coefficient was ~1.5% of the value in dilute buffer; in the nucleus albumin was largely immobile. This indicated that albumin mobility is dominated by association with immobile cellular structures.

Nucleocytoplasmic flux of dextrans depended inversely on molecular mass with an exclusion limit between 17 and 41 kD. This agrees with previous measurements on primary hepatocytes (Peters, R., 1984, *EMBO [Eur. Mol. Biol. Organ.] J.* 3:1831–1836), suggesting that in both cell types the nuclear envelope has properties of a molecular sieve with a functional pore radius of ~55 Å.

In the eukaryotic cell gene expression is regulated on various levels. Transcription, processing, and translation have been extensively studied (5), but the role of nucleocytoplasmic transport has remained a mystery (18). In the case of exogeneous substances, i.e., compounds that are not regular internal components of the cell but introduced by microinjection or other means, it is a common feature that small molecules can easily penetrate through the nuclear envelope whereas larger ones are excluded. The exclusion limit of the nuclear envelope is such that many of the endogeneous molecules involved in the regulation of gene activity or in the transfer of genetic information from nucleus to cytoplasm would not be able to pass through the nuclear envelope passively. This clearly implies the existence of specific transport mechanisms. Recently, the first features of the molecular basis that may underlie specific nucleocytoplasmic transport have emerged. For instance, in the case of nucleoplasmin, a protein found in high concentrations in the nucleus of *Xenopus* oocytes, it was shown (6) that the nuclear location signal resides in an external part of the protein, the "tail," which can be isolated and studied separately. In the case of the SV40 T antigen a short amino acid sequence has been identified (12, 15) specifying nuclear location; strikingly, substitution of a single amino acid residue (lysine 128) abolished accumulation in the nucleus.

In the past, studies of nucleocytoplasmic transport were frequently conducted with unusually large cells such as amphibian oocytes because autoradiography, microdissection, and tracer techniques could be applied. We have recently extended the method of fluorescence microphotolysis (FM)[1] to the study of membrane transport in single, normal-sized, somatic cells (21–23). FM, also referred to as photobleaching, was originally introduced (27) for the measurement of translational diffusion in the membranes of single cells and has been widely applied in that field (1, 4, 20, 31). In the version used for flux measurement, FM permits the quantitative assessment of membrane transport of fluorescent solutes in single cells. A high time resolution and sensitivity, the requirement of only extremely small amounts of substances and cells, and the possibility of measuring transport within the living cell are some characteristic features of the method (for review see reference 24). So far transport across the nuclear envelope has been studied by FM in hepatocytes (23), isolated liver cell nuclei (21), and nuclear ghosts (16).

In the present study, FM has been extended to the measurement of nucleocytoplasmic transport in regular tissue culture cells, namely to hepatoma tissue culture (HTC) cells, a line derived from Reuber hepatoma. Such cells differ from

[1] *Abbreviations used in this paper:* FBSA, fluorescein isothiocyanate–labeled bovine serum albumin; FD, fluorescein isothiocyanate–labeled dextran; FM, fluorescence microphotolysis; HTC, hepatoma tissue culture; PEG, polyethylene glycol.

most fully differentiated primary cells in that they have a much larger nucleocytoplasmic volume ratio. Hence, the cytoplasmic pool is relatively small. Experimental difficulties associated with this situation were overcome by formation of polykaryons. Translational mobility and nucleocytoplasmic transport were measured for various fluorescently labeled dextrans because these molecules are hydrophilic, spherical, have little tendency to be bound or degraded within cells, and are available as a homologous series with molecular mass ranging from a few to several hundred kilodaltons (19). For comparison a protein, bovine serum albumin (BSA), was included in the study. It was observed that the passive permeability of the nuclear envelope in hepatoma cells is similar to that in primary hepatocytes.

FM has been previously employed to measure the translational mobility of proteins in the cytoplasm of cultured cells and of amebae (11, 14, 30, 32). A rather strong restriction of mobility with no apparent dependence on molecular size was observed. The systematic measurements presented in this article reveal, however, that the mobility of dextrans in both cyto- and nucleoplasm depends inversely on molecular size and thus, in a surprisingly simple manner, seems to follow the Stokes-Einstein relationship. On this basis, values for the viscosity of the intracellular aqueous phase in nucleus and cytoplasm are deduced. In accordance with the quoted previous studies (11, 37) the cytoplasmic mobility of BSA was observed to be strongly restricted and could not be explained by viscosity effects alone. In the nucleus, BSA mobility had not been measured previously. The present article shows that BSA was almost completely immobile in the nucleus.

Materials and Methods

Chemicals

Fluorescein isothiocyanate-labeled dextrans FD10, FD20, FD40, FD70, and FD150 and fluorescein isothiocyanate-labeled BSA (FBSA) were obtained from Sigma Chemie (Deisenhofen, Federal Republic of Germany). FD3 was from Deutsche Pharmacia (Freiburg, Federal Republic of Germany). Mean molecular masses, translational diffusion coefficients, and Stokes radii of these substances are given in Table I.

Cells

HTC cells, a derivative of Morris hepatoma 7288C, were obtained from Flow Laboratories (Bonn, Federal Republic of Germany). Cells were grown in Dulbecco's modified Eagle's medium with 10% fetal calf serum and 2% glutamine. For microscopic studies cells were plated in 60-mm-diam plastic dishes.

Table I. Physical Data of Microinjected Molecules

Abbreviation	Mean molecular mass	Diffusion coefficient* in buffer	Stokes radius‡
	kD	$\mu m^2/s$	*Å*
FD3	2.9	97.8 ± 6.0	22.0
FD10	10.5	75.7 ± 2.5	28.3
FD20	17.5	65.1 ± 6.5	33.0
FD40	41.0	46.3 ± 4.6	46.4
FD70	62.0	39.0 ± 2.6	55.1
FD150	156.9	23.7 ± 1.3	90.7
FBSA	67	65 ± 6	33

* Dextran data pertain to 1 μM solution in 7 mM phosphate buffer, pH 7.4, 20°C (reference 21). FBSA data are from reference 3.

‡ Molecular radius r was calculated according to $r = (k\ T)/(6\ \pi\ \eta\ D_{free})$, where k is Boltzmann's constant, T is absolute temperature, η is solvent viscosity, and D_{free} is the translational diffusion coefficient in dilute buffer.

Fusion

Polykaryons were produced following a suggestion of Grässmann et al. (9). Polyethylene glycol, (PEG), mean molecular mass 1.5 kD, was obtained from Roth KG (Karlsruhe, Federal Republic of Germany) and dissolved in Dulbecco's modified Eagle's medium to give a 50% (wt/vol) solution. Confluent HTC monolayers were fused by removing the medium and adding 1.5 ml of the PEG solution per 60-mm petri dish. After 30 s the PEG solution was removed, and cells were washed three times with medium and kept over night in the incubator.

Microinjection

Normal, mononuclear HTC cells and PEG-induced polykaryons were injected directly before microscopic measurements as described (23).

Fluorescence Microphotolysis and Video-Intensification Microscopy

FM instrumentation was essentially as described (26). An image processing system (model 1966-12; Hamamatsu Photonics Europa, Seefeld, Federal Republic of Germany) was added to the microscope and used to directly follow microinjection at low levels of fluorescence excitation and to obtain photographs from injected cells. Diffusion measurements were performed employing a homogeneously irradiated area of 3.15-μm radius and evaluated according to Axelrod et al. (2):

$$D = (0.88\ a^2)/(4\ t_{1/2}), \quad (1)$$

where D is the translational diffusion coefficient, a is the radius of the irradiated area, and $t_{1/2}$ is the half-time of fluorescence recovery. The mobile fraction R_M was determined from

$$R_M = [F(\infty) - F(0)]/[F(-) - F(0)] \quad (2)$$

where F(−), F(0), and F(∞) are fluorescence signal before, immediately after, and very long after photolysis, respectively. Flux measurements were performed as described (23) employing an irradiated area of 7.9-μm radius, which approximately corresponds to the average radius of HTC nuclei (8–10 μm). As previously (23), a 40-fold, numerical aperture 0.75 water immersion objective lens was used. Under these conditions the laser beam traverses the cell as a cylinder and the depth of focus is larger than the thickness of the cell. Evaluation of flux measurements followed described procedures (21, 23):

$$[F(t) - F(\infty)]/[F(0) - F(\infty)] = e^{-Kt}, \quad (3)$$

where F(t) is fluorescence signal at time t and K is the rate constant of influx. The mobile fraction R_M is given as in diffusion measurements by Eq. 2. The temperature of the cells during FM measurements was controlled to an accuracy of approximately ±0.5°C employing the device described previously (25). Fluorescence scans were obtained by means of a scanning stage (Zeiss, Oberkochen, Federal Republic of Germany); the laser beam was focused to a 1.25-μm-diam spot and cells were scanned on a linear pathway through the beam in 0.5-μm steps.

Results

Advantage in Flux Measurements of Employing Polykaryons Instead of Mononucleated Cells

An example of the measurement of nucleocytoplasmic flux in normal, mononucleated HTC cells is shown in Fig. 1 *a*. FD3 was injected into the cytoplasm of the cell and fluorescence was measured in the nuclear region. Then, by increasing the intensity of irradiation ~10,000-fold for a short time (1/30 s), most of the fluorophores in the nuclear region were irreversibly photolysed and thus rendered nonfluorescent. Subsequently, the initial low beam power was restored and the entry into the photolysed region of fresh fluorophores was monitored by fluorescence measurement. Fluorescence was observed to recover quickly. However, the initial fluorescence level was never restored. Usually, the new equilibrium was ~50% of the initial one. Similarly, when the cell was subjected

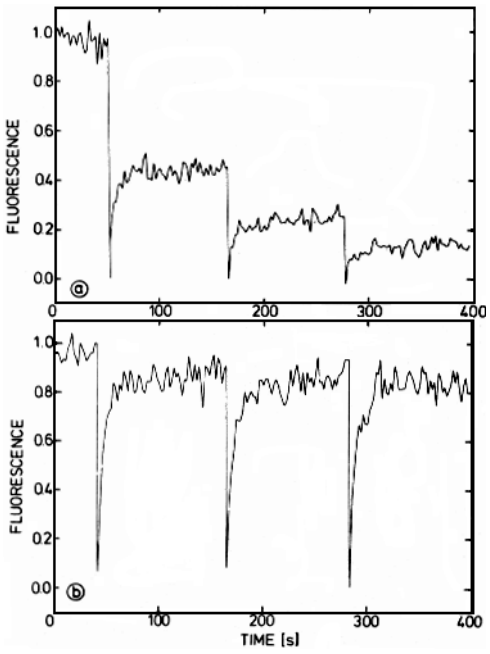

Figure 1. Measurement of nucleocytoplasmic flux in (*a*) normal HTC cells and (*b*) PEG-induced polykaryons. The ordinate gives normalized fluorescence in terms of [F(t) − F(0)]/[F(−) − F(0)] where F(−), F(0), and F(t) are fluorescence before, immediately after, and at time *t* after photolysis, respectively. Cells were injected with a small dextran (FD3) and then photolysed three times in succession. (*a*) In normal HTC cells fluorescence recovery was incomplete because, by photolysing the nucleus, a major part of the cellular pool of fluorescent solute was rendered nonfluorescent. (*b*) In polykaryons fluorescence recovery was 90% complete after the first photolysis and 100% complete after the second and third photolyses. This indicated that ~90% of the dextran was mobile and that the cytoplasmic pool was not depleted by photolysis of the nucleus.

to a second and third photolysis the new equilibrium level was always only ~50% of the preceding one. This behavior had to be expected considering the large nucleocytoplasmic volume ratio characteristic of tissue culture cells. Thus, when the nucleus is photolysed, most of the fluorophores in the cell are rendered nonfluorescent, and with each additional photolysis the pool of fluorophores is reduced by the same proportion. The actual nucleocytoplasmic volume ratio can be roughly estimated from fluorescence scans of cells injected with FD3 (not shown; for a corresponding scan of a polykaryon injected with a large dextran see Fig. 3; for a scan of a primary hepatocyte injected with FD3 see Fig. 3 of reference 23). FD3 seemed to distribute freely in the cell; e.g., no indication of an exclusion from or an accumulation in the nucleus was found. Therefore, a scan of intracellular FD3 fluorescence, to a first approximation, is a relative measure of the geometric cellular profile (23). During photolysis the laser beam traversed the cell as cylinder covering most of the diameter of the nucleus. In this manner we estimate that from one-quarter to one-half of the cellular FD3 pool would be consumed by each photolysis, which is in good agreement with measurements such as shown in Fig. 1.

The situation is different in polykaryons. When many cells merge to form a sometimes very large polykaryon one nucleus assumes only a negligibly small fraction of the total cell volume. Photolysis of one nucleus therefore does not noticeably deplete the cytoplasmic pool, and, provided the fluorophores can enter the nucleus and are completely mobile, nuclear fluorescence should recover after photolysis to the initial level. A corresponding experiment is displayed in Fig. 1*b*. FD3 was injected into the cytoplasm of a polykaryon obtained by PEG-induced fusion of confluent HTC cells. After the first photolysis fluorescence recovered to 80–90% of the initial level. After the second and third photolysis 100% recovery was observed. This revealed that 80–90% of the fluorophores were mobile on the time scale of the experiment and that nuclear volume was negligibly small as compared with cell volume.

Properties of HTC Polykaryons

The light microscopic appearance of normal HTC cells and PEG-induced polykaryons is illustrated in Fig. 2. The degree of fusion varied between wide limits. Sometimes polykaryons formed from many hundred cells. More frequently, fused cells with 2–10 nuclei were observed (Fig. 2, *c–h*); such oligokaryons were used for microinjection and FM measurements. The nuclei were found to gather sometimes in the center of the cell (Fig. 2*b*) or to remain dispersed (e.g. Fig. 2, *c* and *e*). Upon injection into the cytoplasm two classes of dextrans could be distinguished: FD3, FD10, and FD20 penetrated into the nucleus (Fig. 2, *c* and *d*), whereas FD40, FD70, and FD150 were excluded from the nucleus (Fig. 2, *e* and *f*). FBSA was also excluded from the nucleus (Fig. 2*g*). If the substances were injected into the nucleus the same permeation behavior was observed; Fig. 2*h* gives an example in which FD70 was injected into one nucleus, a small amount of FD70 was spilled into the cytoplasm during injection to mark cell contours, and a second nucleus remained without fluorescence.

The relative thickness (vertical diameter) of nuclei and embedding cytoplasmic layer in the nuclear region was estimated from point measurements of polykaryons injected with one of the larger, nonpenetrating dextrans. Fluorescence intensity over the nucleus was compared with that of a region close to the nucleus. In this manner it was estimated that the nucleus assumed 59 ± 7% of cell thickness (mean ± SD of 10 measurements). Another valuable means of estimating nuclear thickness is shown in Fig. 3, which displays a fluorescence scan through a polykaryon injected into the cytoplasm with FD70. The linear scanning path crossed two nuclei. In that cell the cytoplasmic layer embedding the nuclei was (exceptionally) small, perhaps only 15–30% of cell thickness. The scan also revealed that cell thickness can vary considerably over the cross-section of the cell.

Translational Mobility of Dextrans in the Cytoplasm

The translational mobility was determined for the dextrans FD20, FD40, FD70, and FD150; in all cases an irradiated area of 3.15-μm radius and a fluorescence sampling time of ≥20 ms were used.

Diffusion coefficients D are plotted in Fig. 4. The main features were (*a*) a definite dependence on molecular mass; D varied between ~7.8 ± 1.0 $\mu m^2/s$ for FD20 and ~1.6 ± 0.2 $\mu m^2/s$ for FD150; and (*b*) no significant dependence on temperature; in the linear regression analysis of D vs. temperature the slope was near zero for all of the dextrans, extreme values being 0.0157 $\mu m^2/s$ °C for FD20 and −0.0174 $\mu m^2/s$ °C for FD40.

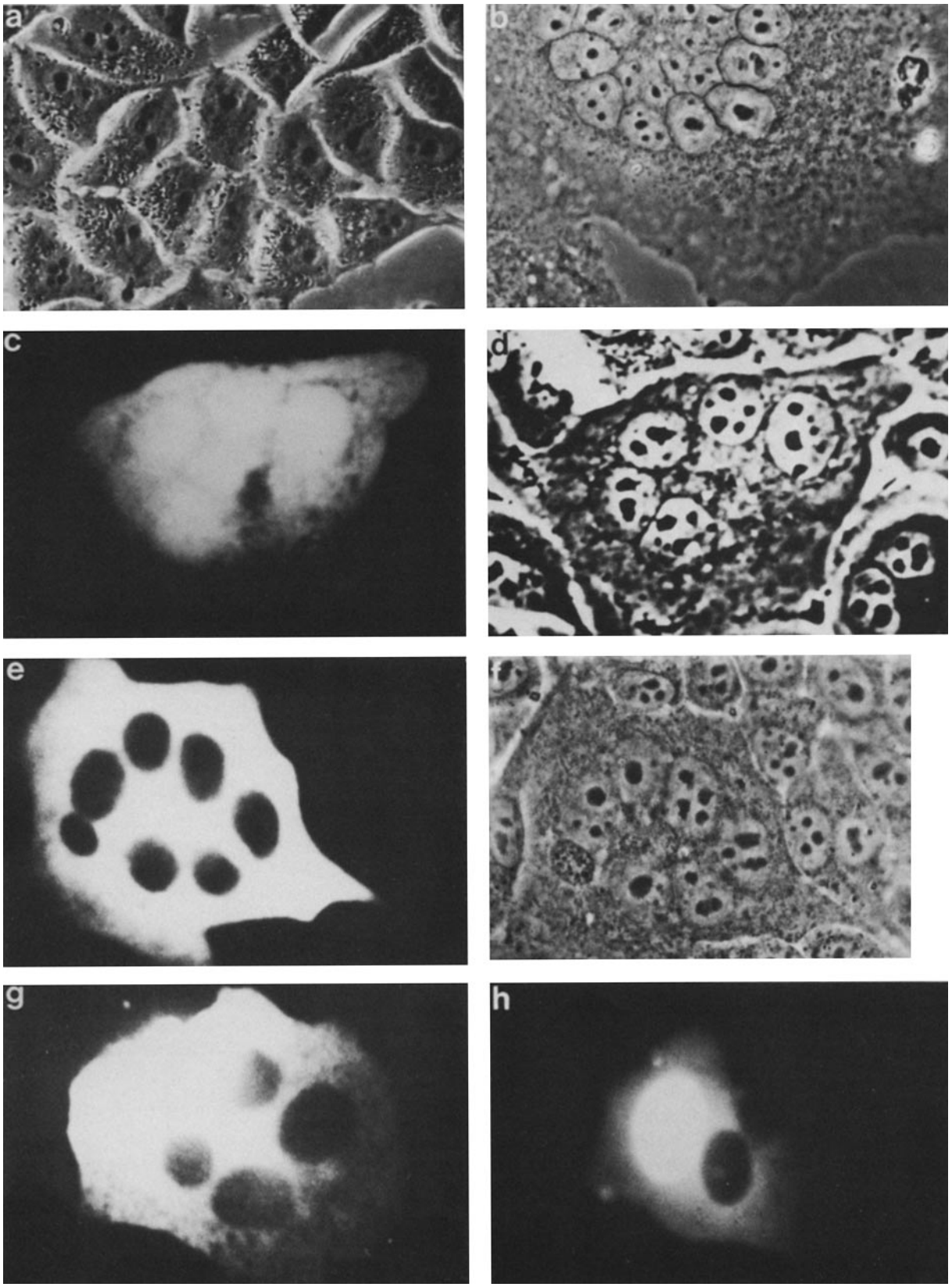

Figure 2. Permeability of the nuclear envelope in HTC polykaryons. (*a*) Phase-contrast micrograph of normal HTC cells. (*b*) Phase-contrast micrograph of a polykaryon. (*c*) Fluorescence micrograph of a polykaryon injected with a small dextran (FD10), which penetrated into the nucleus. (*d*) Phase-contrast micrograph of *c*. (*e*) Fluorescence micrograph of a polykaryon injected with a large dextran (FD70), which was excluded from the nucleus. (*f*) Phase-contrast micrograph of *e*. (*g*) Fluorescence micrograph of a polykaryon injected with BSA. (*h*) Fluorescence micrograph of an intranuclear injection of a large dextran (FD70); a little bit of the dextran was spilled into the cytoplasm to mark the contours of the cell. Dextran did not penetrate into the second nucleus.

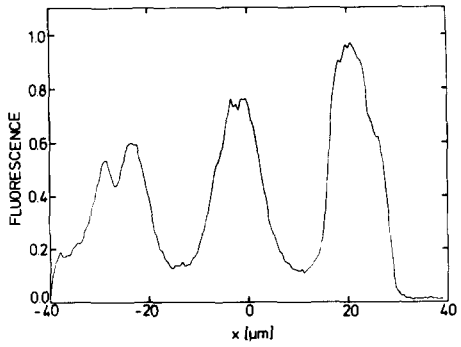

Figure 3. A fluorescence scan through a polykaryon injected with a large dextran (FD70). The scanning path crossed two nuclei.

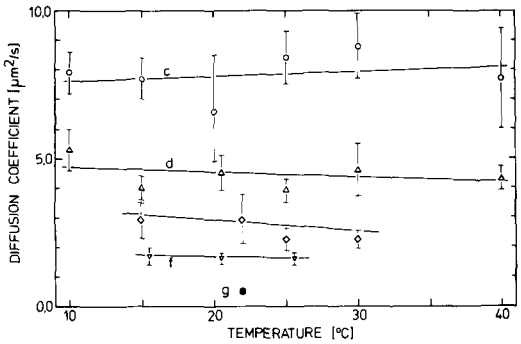

Figure 4. Translational mobility of dextrans and BSA in the cytoplasm of HTC polykaryons. The diffusion coefficient is plotted versus temperature for the dextrans FD20 (curve *c*), FD40 (curve *d*), FD70 (curve *e*), and FD150 (curve *f*), and for BSA (*g*). Data represent the mean ± SD of 18–20 measurements. The straight lines were determined by linear regression.

The mobile fraction R_M was ~0.90 ± 0.05 without apparent dependence on temperature or molecular mass. For example, at 25°C, R_M = 0.93 ± 0.03 (FD20), 0.89 ± 0.6 (FD40), 0.88 ± 0.03 (FD70), and 0.90 ± 0.12 (FD150), respectively. For FD40, R_M = 0.90 ± 0.04 (10°C), 0.93 ± 0.03 (15°C), 0.86 ± 0.06 (20°C), 0.89 ± 0.06 (25°C), 0.92 ± 0.03 (30°C), and 0.95 ± 0.04 (40°C), respectively. Similar R_M values were obtained for other temperatures and dextrans. Mobile and immobile, in the present context, are only meant in relation to the time domain of the measurement, which was 2–20 s. Indeed, if the cell was left in the dark for 10–30 min after photolysis the "immobile" fraction seemed to disappear and fluorescence to recover completely. However, since it is difficult to measure precisely a change in fluorescence that is both slow and small we did not attempt to quantify the kinetics of the "immobile" fraction. Its origin remains obscure. The diffusion coefficients given in this article exclusively relate to the "mobile" fraction and would not be influenced by slow changes of the small "immobile" fraction.

Translational Mobility of Dextrans in the Nucleoplasm

The larger dextrans FD40, FD70, and FD150 were injected into nuclei and their mobility was determined under the same conditions employed in studies of mobility in the cytoplasm. Measurements were only performed on nuclei with radii at least fourfold larger than that of the irradiated area (3.15 µm) and only when intranuclear fluorescence intensity was stable, indicating that the nuclear envelope had resealed after microinjection.

Diffusion coefficients are plotted in Fig. 5. As with cytoplasmic mobility a definite dependence on molecular mass was observed. At 23°C, for instance, D varied between 6.7 ± 0.8 µm²/s for FD40 and 3.8 ± 0.7 µm²/s for FD150. In contrast to cytoplasmic mobility, however, there was an apparently linear dependence of D on temperature. The linear regression analysis yielded values for the slope between 0.101 µm²/s °C for FD150 and 0.066 µm²/s °C for FD70. For a given dextran and a given temperature the diffusion coefficient was 50–100% larger in the nucleus than in the cytoplasm.

The mobile fraction was ~0.82 ± 0.05 without apparent dependence on temperature or molecular mass. For instance, at 22°C, R_M = 0.84 ± 0.04 (FD40), 0.79 ± 0.08 (FD70), and 0.79 ± 0.05 (FD150), respectively. For FD40, R_M = 0.81 ± 0.04 (10°C), 0.84 ± 0.07 (22°C), and 0.83 ± 0.05 (35°C), respectively. Similar R_M values were obtained for other temperatures and dextrans.

Translational Mobility of BSA in Cytoplasm and Nucleus

FBSA displayed a mobility strikingly different from that of dextrans. Examples of measurements of cytoplasmic and intranuclear mobility are shown in Fig. 6. In the cytoplasm the

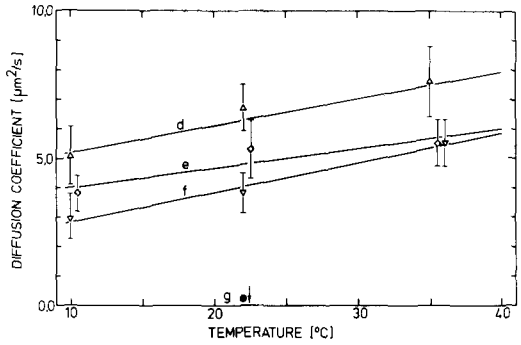

Figure 5. Translational mobility of dextrans and BSA in the nucleus of HTC cells. The diffusion coefficient is plotted versus temperature for the dextrans FD40 (curve *d*), FD70 (curve *e*), and FD150 (curve *f*), and for BSA (in *g*, the arrow indicates that albumin was largely immobile). Data represent the mean ± SD of 12–28 measurements. The straight lines were determined by linear regression.

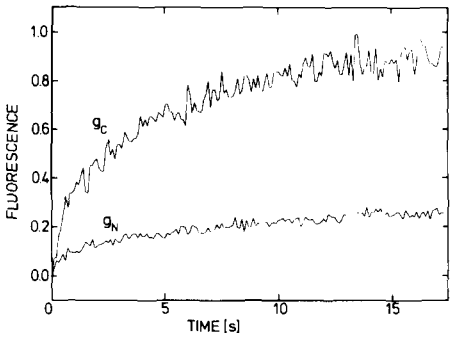

Figure 6. Mobility measurement of BSA in the cytoplasm (g_C) and in the nucleus (g_N) of HTC polykaryons. The ordinate gives fluorescence in normalized form, as in Fig. 1; photolysis was at t = 0 s. The cytoplasmic curve corresponds to a diffusion coefficient of 1.0 µm²/s. In the nucleus albumin was >80% immobile.

apparent diffusion coefficient of FBSA was 1.0 ± 0.2 $\mu m^2/s$ at 23°C (mean ± SD of 19 measurements), i.e., it was markedly smaller than that of the largest dextran (compare Fig. 4, point *g*). The mobile fraction was similar to that of the dextrans, namely 0.85 ± 0.07. In contrast, FBSA was immobile to >80% in the nucleus (Fig. 6, curve *g*).

Nucleocytoplasmic Flux of Dextrans

Flux measurements were performed in the following manner. One of the smaller dextrans (FD3, FD10, or FD20) was injected into the cytoplasm of a polykaryon. After the dextran had distributed between cytoplasm and nucleus, fluorescence was measured in the nucleus using an irradiated area of 7.9-μm radius. Then, fluorophores were photolysed by a high-intensity light pulse and influx was monitored at the initial low beam power. In the case of nonpenetrating dextrans an upper limit of the influx rate constant was determined without photolysis: the dextran was injected into the cytoplasm; after a gap of 15–30 s (necessary to withdraw the pipette and perform adjustments) fluorescence was measured first in the cytoplasm at a position close to the nucleus and then over the nucleus; at the end of the experiment fluorescence was again measured in the cytoplasm to ensure that the cell was tight.

Sample measurements of nucleocytoplasmic flux are given in Fig. 7. The kinetics of fluorescence recovery depended strongly on molecular radius *r* with an exclusion limit between $r = 33$ Å and 46 Å, i.e., FD20 and FD40. Similar results were obtained previously with primary hepatocytes (23). However, the data of the present study also revealed a difference between hepatocytes and hepatoma cells. Whereas flux curves of hepatocytes (23) and other systems (25) are well described by Eq. 3 the hepatoma data could not be fitted sufficiently well by a single-exponential term (data not shown). Clearly, the hepatoma flux curves had at least two components. In Fig. 7, for instance, the experimental data were fitted by a linear combination of two single-exponential terms (full lines). The origin of the bi- or multiphasic nature of the flux curves is unresolved but may well have simple geometric reasons. Eq. 3 holds in the case of passive membrane transport and very fast diffusion in both external and internal compartments (22). In HTC cells the nuclei are not spherical but very flat and ellipsoid so that diffusion pathways in the cytoplasmic layer embedding the nucleus are long. Therefore, the initial fast phase could be due to diffusion in the cytoplasm. This contention is supported by measurements of diffusion in the cytoplasm (data not shown). When the same size of the irradiated area as in flux measurements (radius 7.9 μm) was used, the fluorescence recovery curves had half-times of a few seconds, in agreement with the fast phase of the flux curves.

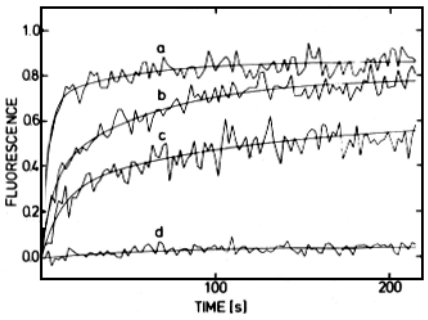

Figure 7. Size dependence of nucleocytoplasmic flux in HTC polykaryons. The ordinate gives fluorescence in normalized form, as in Fig. 1; photolysis was at $t = 0$ s. Curves *a–d* pertain to the dextrans FD3, FD10, FD20, and FD40, respectively.

Discussion

A major objective of the present study was to establish a method to measure nucleocytoplasmic flux in permanent cell lines. We have previously shown (23) that fluorescence microphotolysis can be used to measure nucleocytoplasmic flux in single primary hepatocytes. Those cells are fully differentiated and have a small nucleocytoplasmic volume ratio (1/20–1/10). The extension of the method to permanent cell lines was not straightforward because tissue culture cells usually display a large nucleocytoplasmic volume ratio (1/3 to 1/2). Therefore, when the nucleus in a typical tissue culture cell is photolysed, most of the cellular pool of fluorescently labeled molecules is rendered nonfluorescent, and fluorescence can only recover to an equilibrium value much smaller than that before photolysis. Of course, such curves (e.g., Fig. 1*a*) could also be evaluated in terms of membrane transport coefficients. Indeed, the time course of fluorescence recovery should follow the same equation as in the case of an infinitely large cytoplasmic pool (Eq. 3). The crucial difference is that with an infinitely large cytoplasmic pool the influx rate constant *K* is given by

$$K = (S_N/V_N)P, \tag{4}$$

where S_N and V_N are surface area and volume, respectively, of the nucleus. If nucleus and cytoplasm are of comparable volume, *K* is given by

$$K = [S_N(1/V_N + 1/V_C)]P, \tag{5}$$

where V_C is cytoplasmic volume. Thus, V_C enters into *K* and increases its variability. A further, and rather serious, disadvantage is the difficulty of discriminating between a volume effect and an immobile fraction: both give rise to incomplete fluorescence recovery. In principle, a discrimination could be based on repeated photolysis. In practice, however, this method would probably not work because the cellular pool of fluorescent molecules is rapidly exhausted (see Fig. 1*a*). We have overcome such difficulties experimentally.

Molecular sieving is a well-documented property of the nuclear envelope (7, 17, 19, 28). For various large cells, mostly amphibian oocytes, through the use of various methods it has been consistently observed that small exogeneous molecules easily penetrate from cytoplasm to nucleus, whereas large molecules are excluded from the nucleus. For frog oocytes Paine et al. (19) measured nucleocytoplasmic flux of dextrans by cryofixation and autoradiography and calculated a functional pore radius of ~45 Å for the nuclear envelope. In the present study nucleocytoplasmic flux has been measured for the first time in a tissue culture cell. The outcome fully confirms the notion that the nuclear envelope has properties of a molecular sieve. Interestingly, molecular sieving is very similar in HTC cells and primary rat hepatocytes (23). In both cells a sharp exclusion limit occurs between FD20 and FD40. In case of hepatocytes the flux data have been used to calculate a functional pore radius of 50–56 Å; a very similar value is consistent with the present results on HTC cells. Also, by a different argument, the present study supports the notion

that nucleocytoplasmic flux of dextrans is a passive process: FD10 influx was not significantly different at 10, 25, and 37°C (data not shown); rate constants agreed within a factor of about two. If nucleocytoplasmic flux were a metabolically driven process, a stronger temperature dependence would be expected. However, because of the experimental uncertainty we cannot completely rule out a small or moderate temperature dependence.

Diffusion in the cytoplasm of living cells has been a matter of interest, speculation, and experimentation for a long time (8, 10, 11, 13, 14, 18, 29, 30, 32), whereas studies of diffusion in the nucleus are of recent origin (23). In general, for a given substance the cytoplasmic diffusion coefficient D_C is smaller than the diffusion coefficient D_{free} in water or buffer. However, the degree of restriction varies greatly and it seems that on a qualitative level two classes with weak and strong restriction, respectively, can be discriminated. For instance, the relative diffusion coefficient D_{rel} (i.e., D_C/D_{free}) of water is 0.2 in human red cells and 0.15 in yeast (29); for inulin in frog oocytes $D_{rel} = 0.2$ (10), and for various dextrans ranging in molecular mass from 3.6 to 24 kD $D_{rel} = 0.20$–0.27 in frog oocytes (18). On the other hand, D_{rel} is 0.025 ($D_C = 1.7$ $\mu m^2/s$) for BSA in fibroblasts (11, 32). $D_C = 3.5$ $\mu m^2/s$ for ovalbumin in macrophages (30), and $D_C = 0.3$ $\mu m^2/s$ for G-actin in chicken gizzard cells (14). Jacobson and Wojcieszyn (11) have recently employed FM to measure D_C in fibroblasts for a number of proteins ranging in molecular mass from 12 to 440 kD. For all of the proteins D_C falls in the range of 0.9 to 1.7 $\mu m^2/s$ (25°C) without apparent dependence on molecular mass. Indeed, the smallest protein (insulin) has the smallest D_C. It was therefore concluded (11) that mobility of proteins in the cytoplasm is dominated by dynamic association with immobile structures rather than by steric restriction. With some plausible assumptions concerning the free energy of association, it was estimated that at any time ~98% of the molecular population is bound (11). Our results, showing that cytoplasmic diffusion of FBSA is strongly restricted in HTC cells ($D_C = 1.0 \pm 0.2$ $\mu m^2/s$, 23°C), support the notion that proteins injected into the cytoplasm can be subject to extensive interactions with immobile cellular components. This interaction is overwhelmingly strong in the nucleus, where FBSA was largely immobile.

In general, it is difficult to derive cyto- or nucleoplasmic viscosity from mobility measurements because at least three, usually interdependent, parameters are involved: association with immobile structural elements, steric hindrance, and viscosity effects. It appears, however, that the situation is largely simplified in case of dextrans, a class of uncharged, hydrophilic, spherical, and rather inert molecules. A molecular association with structural elements should concern all of the dextrans to a comparable degree because their chemistry is simple and homogeneous. Probably, a differential interaction with cellular structures would have become apparent in a systematic variation of the immobile fraction ($1\text{-}R_M$) which was not the case. The immobile fraction was relatively small for all dextrans and did not depend on temperature. Steric hindrance of intracellular diffusion could arise from impermeable inclusions such as a microtrabecular lattice, intermediate filaments, microfilaments, microtubules, organelles, or chromatin. However, these inclusions are of supramolecular dimensions and therefore would elongate the diffusional pathway of all macromolecules to the same degree, with no discrimination of molecular size. This type of steric hindrance has been referred to as tortuosity and was used to explain the diffusion coefficient of inulin in the cytoplasm of frog oocytes (Eq. 5 in reference 10). In the diffusion experiments of this study no indication of size discrimination, for instance an exclusion limit, was observed. We therefore assume that the intracellular diffusion of dextrans is mainly determined by two parameters, steric hindrance and viscosity, and that furthermore steric hindrance is constant and affects all of the dextrans to the same extent. If this assumption is true cyto- and nucleoplasmic viscosity can be derived from dextran diffusion by the following simple procedure.

The experimentally determined intracellular diffusion coefficients of the dextrans depended on molecular mass for both cyto- and nucleoplasm (Figs. 4 and 5). A closer look at the data suggested that diffusion coefficients were inversely proportional to molecular radius and might follow a modified Stokes-Einstein equation:

$$D = (kT)/(6\ \pi\ \eta\ r) + b, \qquad (6)$$

where k is Boltzmann's constant, T is absolute temperature, η is solvent viscosity, and r is molecular radius. For the series of dextrans used in this study Fig. 8 gives a plot of D vs. $1/r$. From the slope of the linear regression, viscosity was calculated according to Eq. 6 to be 6.6 cP for the nucleoplasm and 8.1 cP for the cytoplasm. These figures are, in a sense, relative values because the molecular radius r was calculated from D_{free} by application of the (unmodified Stokes-Einstein equation. Thus, the analysis actually indicates that the nucleoplasm is 6.6 times and the cytoplasm 8.1 times more viscous than dilute buffer. These values agree reasonably well with previous determinations, although only a limited set of values is available. In a recent short survey (32) six values of cytoplasmic viscosity were tabulated that range from 2 to 30 cP (most entries are between 3 and 6 cP); no values for nucleoplasmic viscosity are available.

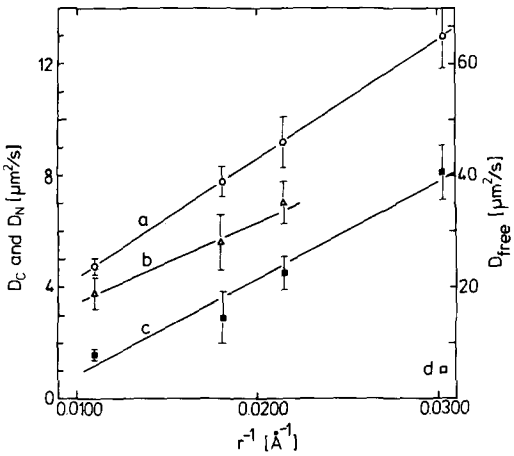

Figure 8. Analysis of dextran mobility in terms of the Stokes-Einstein equation. The translational diffusion coefficients in dilute buffer (D_{free}), in the nucleoplasm (D_N), and in the cytoplasm (D_C) were plotted versus reciprocal molecular radius. Curve *a*, diffusion in buffer; curve *b*, in the nucleoplasm; curve *c*, in the cytoplasm. For comparison the cytoplasmic diffusion coefficient of BSA is also plotted (*d*). T = 23°C. The straight lines were obtained by linear regression and correspond to a viscosity of 1 cP (curve *A*), 6.6 cP (curve *b*), and 8.1 cP (curve *c*).

A marked difference between nucleus and cytoplasm became apparent in the temperature dependence of dextran diffusion. In the nucleus, diffusion coefficients increased by a factor of 1.45–1.86 between 10 and 37°C (Fig. 5). Such a factor is normal for the temperature-dependent viscosity decrease of a concentrated aqueous solution of macromolecules. In contrast, cytoplasmic diffusion coefficients were virtually independent of temperature, suggesting that viscosity changes are balanced by changes in steric parameters and/or association kinetics. Further studies will be necessary to discriminate between these parameters.

We thank Mrs. Daniela Gahl for excellent collaboration and Mrs. Brigitte Lehmann for the drawings.

Support by the Deutsche Forschungsgemeinschaft is gratefully acknowledged.

Received for publication 8 April 1985, and in revised form 21 November 1985.

References

1. Axelrod, D. 1983. Lateral motion of membrane proteins and biological function. *J Membr. Biol.* 75:1–10.

2. Axelrod, D., D. Koppel, J. Schlessinger, E. Elson, and W. W. Webb. 1976. Mobility measurement by analysis of fluorescence photobleaching recovery kinetics. *Biophys. J.* 16:1055–1069.

3. Barisas, B. G., and M. D. Leuther. 1979. *Biophys. Chem.* 10:221–229.

4. Cherry, R. J. 1979. Rotational and lateral diffusion of membrane proteins. *Biochim. Biophys. Acta.* 559:289–327.

5. Darnell, J. E., Jr. 1982. Variety in the level of gene control in eukaryotic cells. *Nature (Lond.).* 297:365–371.

6. Dingwall, C., S. V. Sharnick, and R. A. Laskey. 1982. A polypeptide domain that specifies migration of nucleoplasmin into the nucleus. *Cell.* 30:449–458.

7. Feldherr, C. M. 1972. Structure and function of the nuclear envelope. *Adv. Cell Mol. Biol.* 2:273–307.

8. Frey-Wyssling, A. 1953. Submicroscopic morphology of protoplasm. Elsevier Publishing Co., Amsterdam. 477 pp.

9. Grässmann, A., M. Grässmann, and C. Müller. 1979. Fused cells are suited for microinjection. *Biochem. Biophys. Res. Commun.* 88:429–432.

10. Horowitz, S. B., and L. C. Moore. 1974. The nuclear permeability, intracellular distribution, and diffusion of inulin in the amphibian oocyte. *J. Cell Biol.* 60:405–415.

11. Jacobson, K., and J. Wojcieszyn. 1984. The translational mobility of substances within the cytoplasmic matrix. *Proc. Natl. Acad. Sci. USA.* 81:6747–6751.

12. Kalderon, D., W. D. Richardson, A. F. Markham, and A. E. Smith. 1984. Sequence requirements for nuclear location of simian virus large-T antigen. *Nature (Lond.).* 311:33–38.

13. Keith, A. D., editor. 1979. The Aqueous Cytoplasm. Marcel Dekker, Inc., New York. 230 pp.

14. Kreis, T. E., B. Geiger, and J. Schlessinger. 1982. Mobility of microinjected rhodamin actin within living chicken gizzard cells determined by fluorescence photobleaching recovery. *Cell.* 29:835–845.

15. Lanford, R. E., and J. S. Butel. 1984. Construction and characterization of an SV40 mutant defective in nuclear transport of T antigen. *Cell.* 37:801–813.

16. Lang, I., and R. Peters. 1984. Nuclear envelope permeability: a sensitive indicator of pore complex integrity. *In* Information and Energy Transduction in Biological Membranes. C. L. Bolis, E. J. M. Helmreich, and H. Passow, editors. Alan R. Liss Inc., New York. 377–386.

17. Paine, P. L. 1975. Nucleocytoplasmic movement of fluorescent tracers microinjected into living salivary gland cells. *J. Cell Biol.* 66:652–657.

18. Paine, P. L., and S. B. Horowitz. 1980. The movement of material between nucleus and cytoplasm. *In* Cell Biology, Vol. 4. D. M. Prescott and L. Goldstein, editors. Academic Press Inc., New York. 299–338.

19. Paine, P. L., L. C. Moore, and S. B. Horowitz. 1975. Nuclear envelope permeability. *Nature (Lond.).* 254:109–114.

20. Peters, R. 1981. Translational diffusion in the plasma membrane of single cells as studied by fluorescence microphotolysis. *Cell Biol. Int. Rep.* 5:733–760.

21. Peters, R. 1983. Nuclear envelope permeability measured by fluorescence microphotolysis of single lever cell nuclei. *J. Biol. Chem.* 258:11427–11429.

22. Peters, R. 1984. Flux measurement in single cells by fluorescence microphotolysis. *European Biophysics Journal* 11:43–50.

23. Peters, R. 1984. Nucleo-cytoplasmic flux and intracellular mobility in single hepatocytes measured by fluorescence microphotolysis. *EMBO (Eur. Mol. Biol. Organ.) J.* 3:1831–1836.

24. Peters, R. 1985. Measurement of membrane transport in single cells by fluorescence microphotolysis. *Trends Biochem. Sci.* 10:223–227.

25. Peters, R., and H. Passow. 1984. Anion transport in single erythrocyte ghosts measured by fluorescence microphotolysis. *Biochim. Biophys. Acta.* 777:334–338.

26. Peters, R., and H. P. Richter. 1981. Translational diffusion in the plasma membrane of sea urchin eggs. *Dev. Biol.* 86:285–293.

27. Peters, R., J. Peters, K. H. Tews, and W. Bähr. 1974. A microfluorimetric study of translational diffusion in erythrocyte membranes. *Biochim. Biophys. Acta.* 367:282–294.

28. Reynolds, C. R., and H. Tedeschi. 1984. Permeability properties of mammalian cell nuclei in living cells and in vitro. *J. Cell Sci.* 70:197–207.

29. Tanner, J. E. 1983. Intracellular diffusion of water. *Arch. Biochem. Biophys.* 224:416–428.

30. Wang, Y.-L., F. Lanni, P. L. McNeil, D. Ware, and L. Taylor. 1982. Mobility of cytoplasmic and membrane-associated actin in living cells. *Proc. Natl. Acad. Sci. USA.* 79:4660–4664.

31. Ware, B. R. 1984. Fluorescence photobleaching recovery. *Am. Lab. (Fairfield Conn).* 16:12–21.

32. Wojcieszyn, J. W., R. A. Schlegel, E.-S. Wu, and K. A. Jacobson. 1981. Diffusion of injected macromolecules within the cytoplasm of living cells. *Proc. Natl. Acad. Sci. USA.* 78:4407–4410.